Vector Control of Permanent Magnet Synchronous Motor by a Two-Level SPWM Inverter

Oğuz Tahmaz
Dept. of Electronic Hardware Development
AVL Research & Engineering Turkey
Istanbul, Turkey
oguz.tahmaz@avl.com

Melih Nafi Ekim
Dept. of Power Electronics
Akım Metal R&D Center
Istanbul, Turkey
mnekim@akimmetal.com.tr

Ali Bekir Yıldız
Dept. of Electrical Engineering
Kocaeli University
Kocaeli,Turkey
abyildiz@kocaeli.edu.tr

***Abstract*— This paper presents Vector Control (Field Oriented Control) simulation of Permanent Magnet Synchronous Motor (PMSM). Mains, motor, and 2-level inverter were modeled in MATLAB/Simulink environment. Gate signals for semiconductors were generated with the SPWM method. Park, Clarke transforms, and the PI controller were used in the FOC algorithm. Important waveforms on the inverter and motor models have been examined in detail.**

Keywords — Motor Drive, 2-Level Inverter, SPWM, PMSM, MATLAB, Simulink, Simulation, Modeling, Field-Oriented Control (FOC), Vector Control, PI Controller, Park and Clarke Transformation

I. INTRODUCTION

Nowadays, PMSMs are mostly used in industrial applications and electrical vehicles thanks to their high efficiency, high power factor, precision, simple structure, high power density, and reduced maintenance costs [1].

The permanent magnet synchronous motor (PMSM) has so many advantages compared to other AC machines. The stator current of an induction motor (IM) contains both magnetizing and torque-producing components. PMSM has permanent magnets in the rotor therefore, it does not need magnetizing current through the stator to supply constant air gap flux. Permanent magnets will maintain constant air flux. Stator current will be used only to produce torque. The power factor of PMSM will be higher for the same output and will be more efficient than IM. The wound-rotor synchronous motor (SM) must have DC excitation on the rotor winding. This DC excitation is usually provided by brushes and slip rings. As a result, rotor losses and brush maintenance costs will be reduced [2].

By the introduction of frequency inverters, V/f speed control was presented. Over time, scalar control techniques became available for performance improvements. AC machines are non-linear, motor parameters vary, and have complex dynamics. Controlling the machine with a feedback loop creates stability issues and feedback signals become difficult to process.

In 1929, R. H. Park introduced rotating reference frames [3]. Nevertheless, the idea of FOC formed over time. This idea relies on torque is proportional to the cross product of stator current and flux [4]. Roots of field-oriented control (FOC) started from Germany in the early 1970s. K. Hasse and F. Blaschke's inventions about the vector control [5][6] shown us PMSM motor can be controlled like a separately excited DC motor [7].

Torque generation in the synchronous, or induction motor is very similar as the dc motor. Stator and rotor fields are not orthogonal to each other in ac machines. Great importance of the vector control is driving the ac motor as a dc motor and controlling the field excitation and the torque generating current separately [8]. Thus, FOC is used to achieve the decoupled control of torque and flux producing current components [9]. FOC also has numerous advantages over V/f control. The advantages are given below [10].

- Full torque capability at a wide speed range
- Better dynamic behavior
- Good transient and steady-state performance
- High torque and low current at startup
- Higher efficiency
- Decoupled torque and flux control
- Four-quadrant operation

There are two important coordinate systems for the FOC concept. One of them is called a stationary reference frame located on the stator and the other one is called a rotating reference frame located on the rotor.

Stator currents can be represented by vectors and these currents can be controlled by FOC. Stator currents, which depend on time and speed are projected to the rotor-fixed two-coordinate (d and q coordinates) system by Clarke and Park transformations. The inputs of the Clarke transformation are three-phase motor currents and the outputs are two-phase α, β currents which are located on the stationary reference frame. The inputs of the Park transformation are α, β currents and the outputs are d, q currents which are located on the rotating reference frame. d and q currents are in the dc waveform, unlike phase currents.

Two input references are needed for field-oriented controlled machines. The first one is the torque component which is aligned with the q coordinate and the second one is the flux component which is aligned with d coordinate. Field-orientated control is based on these transformations and its control structure handles instantaneous electrical quantities.

As a result, control will be accurate in steady-state and transient working operations. If the PMSM motor is star-connected and two-phase currents are measured (the third phase current can be calculated according to Kirchoff's current law) then the stator flux position can be estimated. If the rotor position is known then the rotor flux position can be estimated. Precise stator and rotor flux position estimation depend on measurement accuracy [11]. Measurement accuracy depends on current sensor precision [12].

978-1-7281-9090-7/20/$31.00 ©2020 IEEE

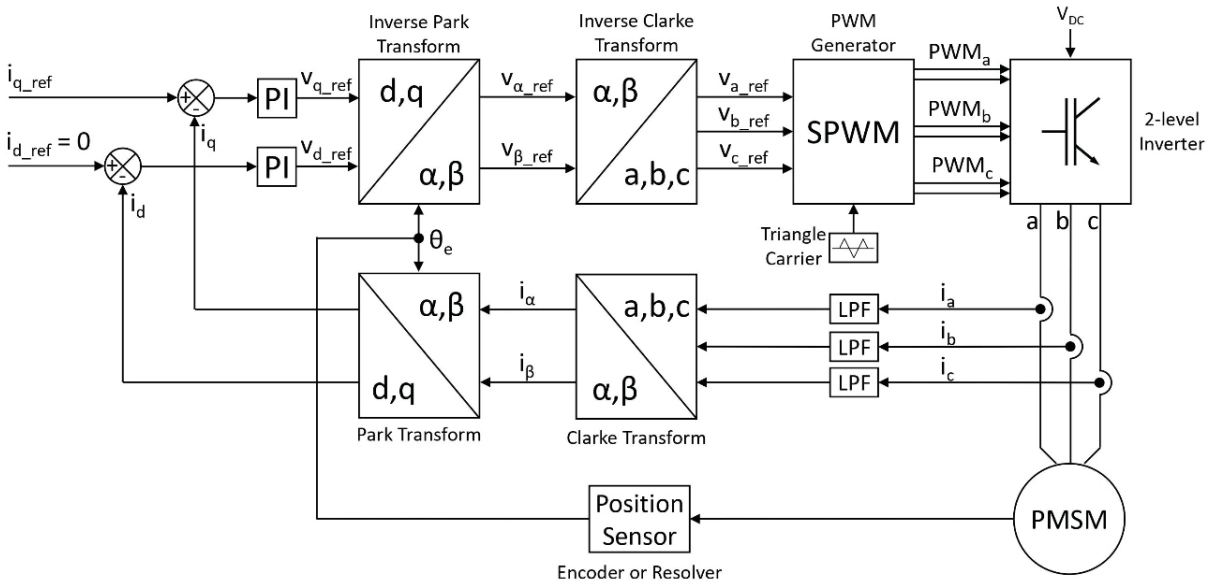

Figure 1. Block Diagram of Vector Control

II. VECTOR CONTROL

A. Field Oriented Control Concept

Separately excited dc motors have good dynamic behavior because armature and field fluxes are orthogonal to each other. Thus, maximum torque is always obtained. Surface-mounted PMSM can be controlled with a similar characteristic (to be operated at the maximum torque point) but the torque and flux components must be obtained separately. Phase currents of three-phase motors are difficult to analyze as they change sinusoidally depending on the position of the rotor. The sinusoidal phase currents in the stator reference frame are converted to dc currents by projecting them to the rotor reference frame with Clarke and Park transformations. A general block diagram of Vector Control is given in figure 1. Summary of all FOC transformations is given in figure 6.

B. Clarke Transform

The Clarke transform (abc to αβ0) is used to simplify the analysis of three-phase circuits. Vector representation of Clarke Transform is given in figure 2. This transformation transforms the signals of three-phase systems to a two-phase system. The following equation (1) is used for the Clarke transformation.

$$\begin{bmatrix} i_\alpha \\ i_\beta \\ 0 \end{bmatrix} = \sqrt{\frac{2}{3}} \begin{bmatrix} 1 & -\frac{1}{2} & -\frac{1}{2} \\ 0 & \frac{\sqrt{3}}{2} & -\frac{\sqrt{3}}{2} \\ \frac{1}{\sqrt{2}} & \frac{1}{\sqrt{2}} & \frac{1}{\sqrt{2}} \end{bmatrix} \begin{bmatrix} i_a \\ i_b \\ i_c \end{bmatrix} \quad (1)$$

C. Park Transform

The Park transformation (αβ0 to dq0) transforms the signals in the two-phase stationary reference frame obtained by the Clarke transformation into a rotational reference frame. The following equation (2) is used for the Park transformation. Vector representation of Park Transform is given in figure 3.

$$\begin{bmatrix} i_d \\ i_q \end{bmatrix} = \begin{bmatrix} \cos\theta & \sin\theta \\ -\sin\theta & \cos\theta \end{bmatrix} \begin{bmatrix} i_\alpha \\ i_\beta \end{bmatrix} \quad (2)$$

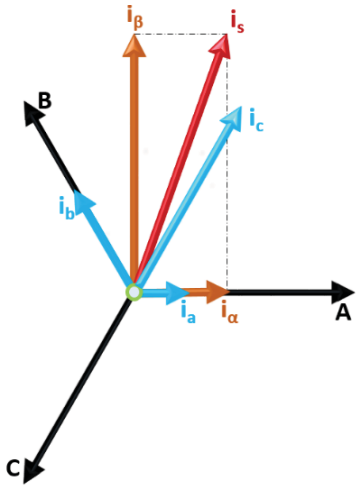

Figure 2. Vector Representation of Clarke Transform

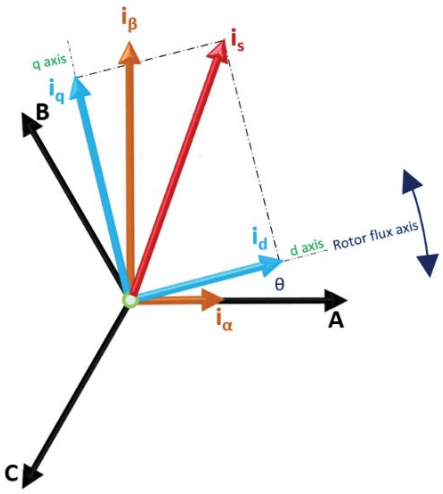

Figure 3. Vector Representation of Park Transform

V_q and V_d voltages are obtained with the PI controller. Input of the PI controller are I_d and I_q currents which are obtained with Clarke and Park transformations.

D. Inverse Park Transform

The inverse Park transformation (dq0 to αβ0) transforms the signals (V_q and V_d voltages) in the rotating reference frame which are obtained with the PI controller into two-phase stationary reference frame. Vector representation of inverse Park transformation is given in figure 4.

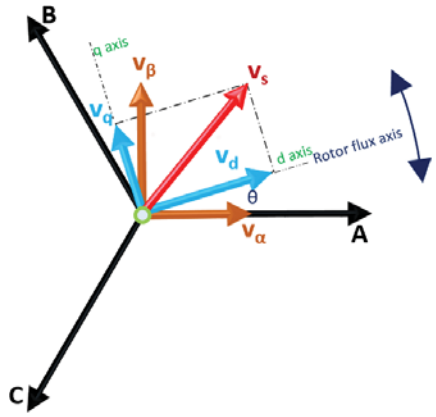

Figure 4. Inverse Park Transform Vector Representation

The following equation (3) is used for the inverse Park transformation.

$$\begin{bmatrix} V_\alpha \\ V_\beta \end{bmatrix} = \begin{bmatrix} \cos\theta & -\sin\theta \\ \sin\theta & \cos\theta \end{bmatrix} \begin{bmatrix} V_d \\ V_q \end{bmatrix} \quad (3)$$

E. Inverse Clarke Transform

The inverse Clarke transformation (αβ0 to abc) transforms the signals in the two-phase rotating reference frame which are obtained with the inverse Park transformation into three-phase stationary reference frame. Vector representation of inverse Clarke transformation is given in figure 5.

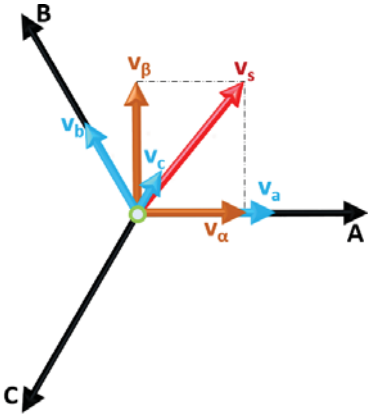

Figure 5. Inverse Clarke Transform Vector Representation

The following equation (4) is used for the inverse Clarke transformation.

$$\begin{bmatrix} V_a \\ V_b \\ V_c \end{bmatrix} = \sqrt{\frac{2}{3}} \begin{bmatrix} 1 & 0 & \frac{1}{\sqrt{2}} \\ -\frac{1}{2} & \frac{\sqrt{3}}{2} & \frac{1}{\sqrt{2}} \\ -\frac{1}{2} & -\frac{\sqrt{3}}{2} & \frac{1}{\sqrt{2}} \end{bmatrix} \begin{bmatrix} V_\alpha \\ V_\beta \\ 0 \end{bmatrix} \quad (4)$$

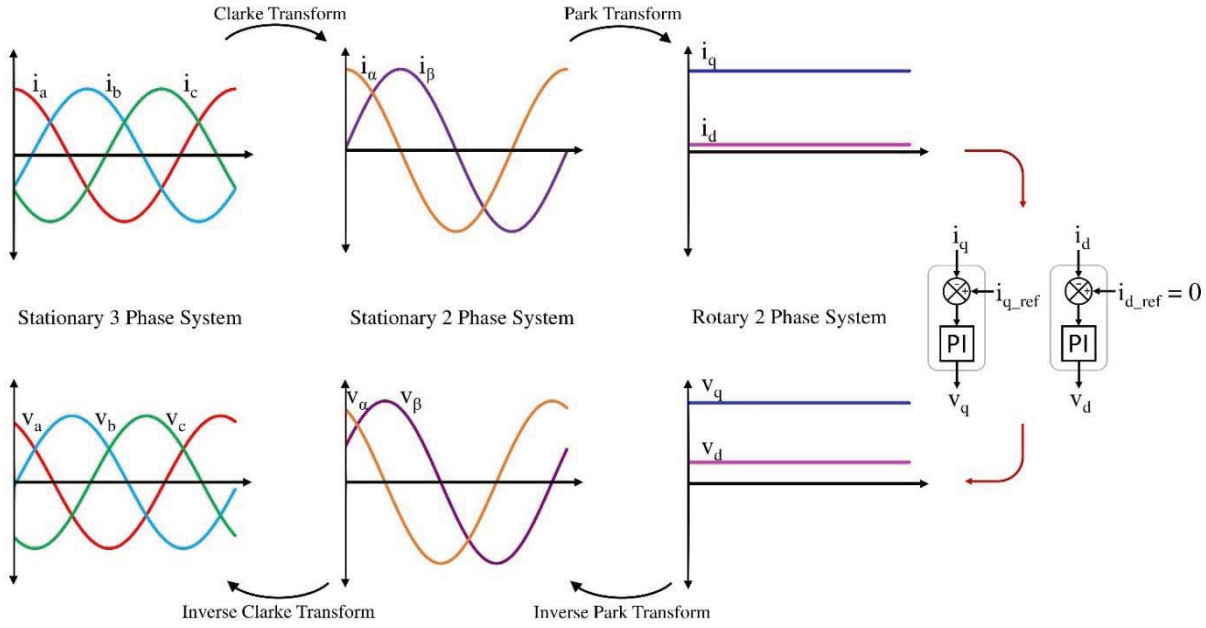

Figure 6. Summary of FOC transformations

III. SWITCHING METHOD

SPWM (Sinusoidal Pulse Width Modulation) is a carrier-based PWM method. Carrier-based PWM methods are the classical and most widely used [13]. In this PWM method, two signals are compared. These signals are called the carrier and modulation signals. The carrier signal is in the triangle waveform. The modulation signal can be in any waveform. In this method, the modulation signal is in the sinusoidal waveform. Switching elements are triggered by the obtained PWM signals.

High side switches will be turned on when the reference signal value greater than the carrier signal. Otherwise, the upper switches will be turned off. High and low side switches work complementary to each other. An example can be seen for high-side switches below in figure 7.

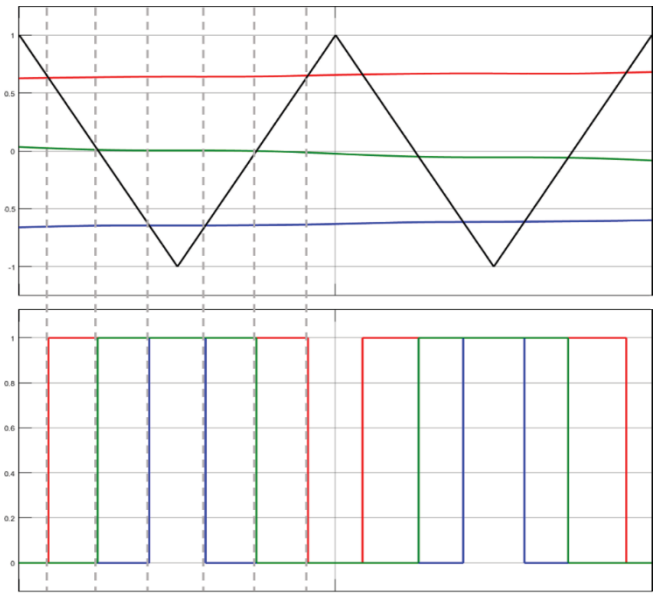

Figure 7. PWM Signal Generation

IV. SIMULATION MODELS

A. Mains, Rectifier and Inverter Model

The mains side is modeled with pure sine wave voltage source, resistor, and inductor. The bulk capacitor is modeled with its equivalent series resistance (ESR). The bulk or the DC link capacitor will be charged through the rectifier. The general model of mains, rectifier, and inverter are given in figure 8. Important parameters related to this part are given in table 1.

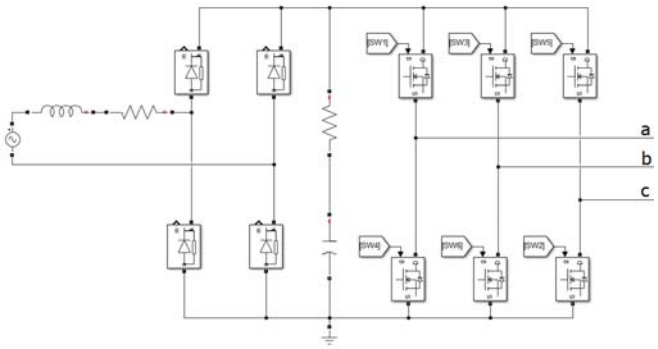

Figure 8. Mains, Rectifier, Inverter Model in Matlab/Simulink

TABLE 1. IMPORTANT PARAMETERS OF MAINS AND BULK CAPACITOR.

Parameters	Description	Value
V_{line}	Mains voltage	220 Vac
L_{line}	Mains inductance	10 µH
R_{line}	Mains resistance	25 mΩ
C_{dc_link}	Capacitance of DC-Link capacitor	1230 µF
R_{esr}	Equivalent series resistance of	50 mΩ

B. Electrical Model of PMSM

The three-phase electrical model of the PMSM consists of three main elements; resistor, inductor, and back EMF. The electrical equivalent circuit model of the PMSM is shown in figure 9.

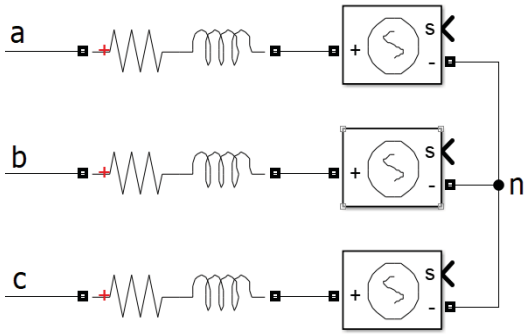

Figure 9. PMSM Motor Electrical Equivalent Model in Matlab/Simulink

The back EMF voltages depend on the back EMF constant, position of the rotor, and angular velocity of the rotor. The back EMF voltages are calculated with (5).

$$\begin{bmatrix} e_a(t) \\ e_b(t) \\ e_c(t) \end{bmatrix} = K_e \omega_m(t) \begin{bmatrix} \cos(\theta_e(t)) \\ \cos\left(\theta_e(t) - \frac{2}{3}\pi\right) \\ \cos\left(\theta_e(t) + \frac{2}{3}\pi\right) \end{bmatrix} \quad (5)$$

The phase-to-neutral voltages depend on the phase currents, back EMF voltages, stator resistances, and stator inductances. The phase-to-neutral voltages are calculated with (6).

$$\begin{bmatrix} v_{an}(t) \\ v_{bn}(t) \\ v_{cn}(t) \end{bmatrix} = \left(R + L\frac{d}{dt}\right) \begin{bmatrix} i_a(t) \\ i_b(t) \\ i_c(t) \end{bmatrix} + \begin{bmatrix} e_a(t) \\ e_b(t) \\ e_c(t) \end{bmatrix} \quad (6)$$

Stator resistance, inductance, and back EMF constant were determined to create the electrical model of the PMSM. Important parameters related to this part are given in table 2.

TABLE 2. PMSM ELECTRICAL MODEL PARAMETERS

Parameter	Description	Value
R_L	Winding Resistance (ph-to-n)	580 mΩ
L_L	Winding Inductance (ph-to-n)	3.75 mH
K_e	Back EMF Constant	24.4 V/krpm

C. *Mechanical Model of PMSM*

The mechanical equivalent circuit model of the motor is given in figure 10.

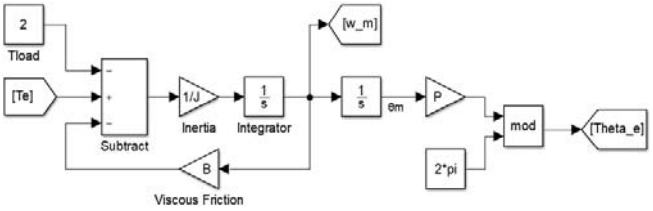

Figure 10. PMSM Mechanical Model in Matlab/Simulink

The mathematical model of the mechanical equivalent circuit of the motor is given in (7) and (8).

$$T_e(t) = J_m \frac{d}{dt}\omega_m(t) + B_m\omega_m(t) + T_L(t) \tag{7}$$

$$\frac{d}{dt}\omega_m(t) = \frac{T_e(t) - T_L(t) - B_m\omega_m(t)}{J_m} \tag{8}$$

Important parameters related to mechanical model of the PMSM are given in table 3.

TABLE 3. PMSM MECHANICAL MODEL PARAMETERS

Parameter	Description	Value
J	Rotor Inertia	0.269e-6 kg.m^2
B	Viscous Friction	5.410e-3 Nm.s
P	Pole Pair	5

D. *Torque Production of Surface Mount PMSM*

Electromagnetic torque generated by a permanent magnet synchronous motor depend on I_d and I_q [16]. Related formula is given in (9).

$$T_e(t) = \frac{3}{2}\frac{P}{2}\lambda_m i_q + (L_d - L_q) i_d i_q \tag{9}$$

One of the very important feature for surface-mounted machine is $L_d = L_q$ equality because stator inductances are independent of rotor position. The second term in equation 9 will be equal to zero [14]. Therefore, direct-axis current does not affect torque. Minimum stator current will be obtained at a constant torque when $i_d = 0$. As a result, electromagnetic torque can be obtained with (10), (11), and (12).

$$T_e(t) = \frac{3}{2}\frac{P}{2}\lambda_m i_q \tag{10}$$

$$\frac{3}{2}\frac{P}{2}\lambda_m = K_t \tag{11}$$

$$T_e(t) = K_t i_q \tag{12}$$

V. SIMULATION OUTPUTS

A. *Mains Side Waveforms*

Mains voltage, mains current, and DC bus voltage are shown in figure 11. It is seen that current is drawn from the mains when the DC bus voltage drops below the mains voltage.

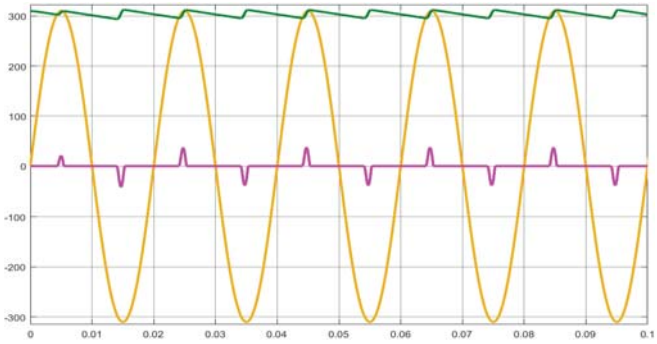

Figure 11. Mains Side Waveforms (V_{line}, I_{line} ,V_{dc_link})

B. *Inverter Side Waveforms*

The three-phase output currents of the inverter, the αβ and dq currents obtained from Clarke and Park transformations are shown in figure 12 respectively.

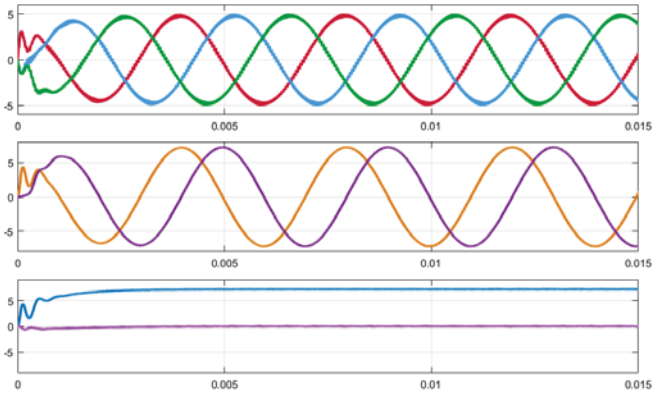

Figure 12. Clarke - Park Transformation Results

The V_d and V_q voltages are transformed to V_α and V_β voltages by inverse Park transformation. V_α and V_β voltages are transformed into voltages V_a, V_b, and V_c by the inverse Clarke transformation. Transformations of these signals can be seen in figure 13 respectively.

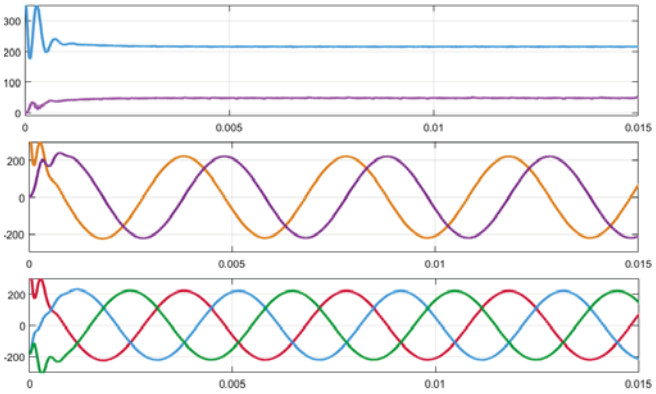

Figure 13. Inverse Park-Clarke Transformation Results

The phase currents are given in figure 14.

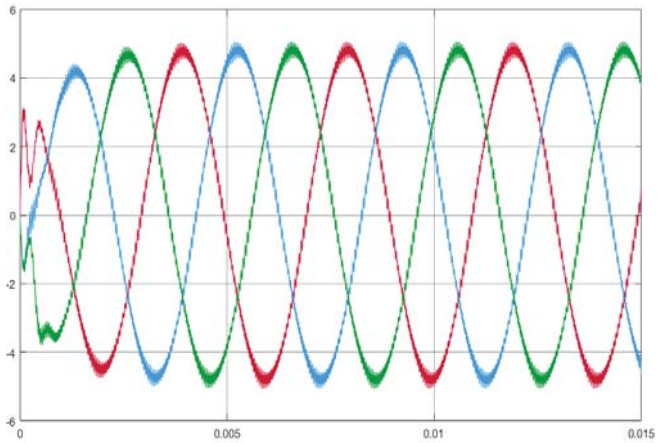

Figure 14. Phase Currents of PMSM (I_a, I_b, I_c)

The sinusoidal reference signals in the sine-triangle comparator (SPWM Method) are waveforms that determine the fundamental frequency of motor currents.

However, in closed loop control, the frequency of the sinusoidal reference signal is affected by the angular velocity of the rotor and the number of motor poles.

The phase-to-neutral voltages are given in figure 15.

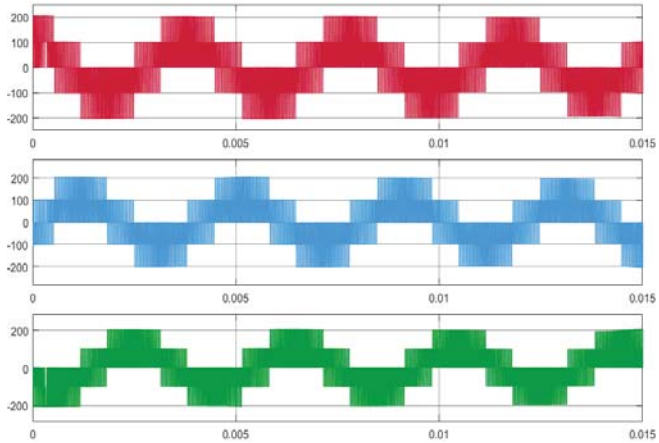

Figure 15. Phase-to-Neutral Voltages of PMSM (V_{an}, V_{bn}, V_{cn})

The phase-to-phase voltages are given in figure 16.

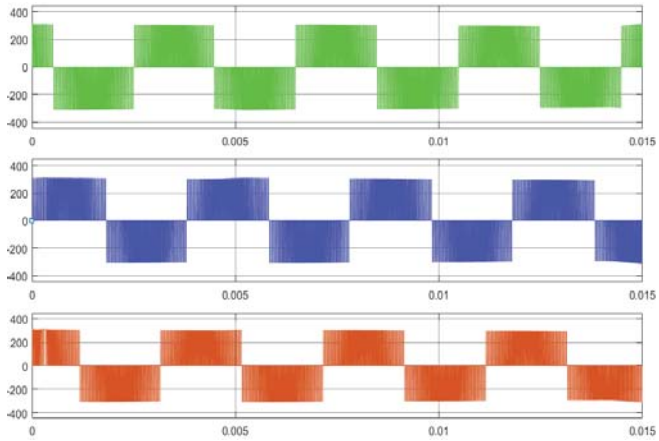

Figure 16. Phase-to-Phase Voltages of PMSM (V_{ab}, V_{ac}, V_{bc})

C. *Field Orientation*

The fact that the motor phase current and the back EMF voltage waveforms shown in figure 17 are in same phase or the phase difference is too small indicates that the field orientation or vector control is operating successfully.

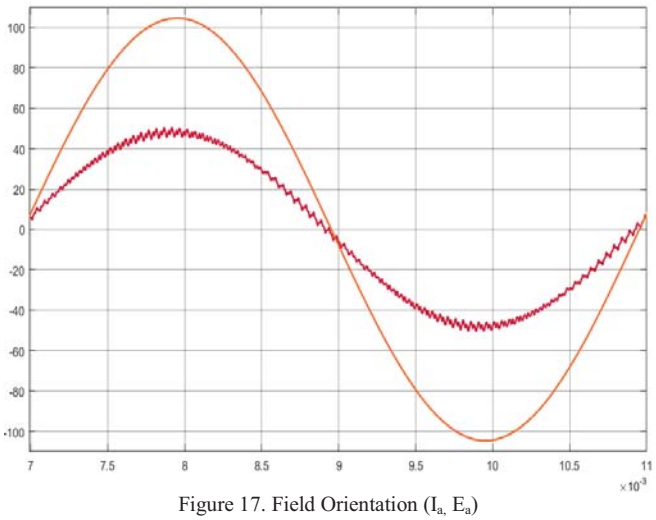

Figure 17. Field Orientation (I_a, E_a)

VI. RESULT

In this study, vector control of surface mount permanent magnet synchronous motor is discussed. Field oriented control algorithm, SPWM method, motor model, inverter model, mains model, and simulation outputs are given in detail. All models are explained with mathematical equations.

The fact that torque can be controlled by the stator currents show that the models created in MATLAB / Simulink environment work in harmony with the Field Oriented Control algorithm.

ACKNOWLEDGMENT

We would like to thank all academicians and engineers for their endless efforts in the development of science and technology.

REFERENCES

[1] Tahmaz, O , Yıldız, A . (2020). Simulation of Permanent Magnet Synchronous Motor Driven by a Two-Level SPWM Inverter . Avrupa Bilim ve Teknoloji Dergisi , () , 21-29 . DOI: 10.31590/ejosat.801868

[2] P. Pillay and R. Krishnan, "Modeling, simulation, and analysis of permanent-magnet motor drives. I. The permanent-magnet synchronous motor drive," in IEEE Transactions on Industry Applications, vol. 25, no. 2, pp. 265-273, March-April 1989, doi: 10.1109/28.25541.

[3] R. H. Park, "Two-reaction theory of synchronous machines generalized method of analysis-part I," in Transactions of the American Institute of Electrical Engineers, vol. 48, no. 3, pp. 716-727, July 1929, doi: 10.1109/T-AIEE.1929.5055275.

[4] J. Bocker and S. Mathapati, "State of the Art of Induction Motor Control," 2007 IEEE International Electric Machines & Drives Conference, Antalya, 2007, pp. 1459-1464, doi: 10.1109/IEMDC.2007.383643.

[5] K Hasse, "Zur dynamik drehzahigeregelter antriebe mit stromrichtergespeisten asynchron-kurzschlublaufermaschinen," Ph.D.dissertation, Tech. Hochschule Darmstadt, July1969.

[6] F. Blaschke, "A new method for the structure decoupling of ac induction machines", 2nd IFAC on multivariable tec. Control syst, pp. 11-13, 1971-Oct.

[7] B. K. Bose, "High performance control and estimation in AC drives," Proceedings of the IECON'97 23rd International Conference on Industrial Electronics, Control, and Instrumentation (Cat. No.97CH36066), New Orleans, LA, USA, 1997, pp. 377-385 vol.2, doi: 10.1109/IECON.1997.671764.

[8] T. Kume and T. Iwakane, "High-Performance Vector-Controlled AC Motor Drives: Applications and New Technologies," in IEEE Transactions on Industry Applications, vol. IA-23, no. 5, pp. 872-880, Sept. 1987, doi: 10.1109/TIA.1987.4504997.

[9] Microsemi, “Field Oriented Control of Permanent Magnet Synchronous Motors / User’s Guide”

[10] V. K. Pavuluri, X. Wang, J. Long, G. Zhuo and W. Lian, "Field Oriented Control of Induction Motors Using Symmetrical Optimum Method with Applications in Hybrid Electric Vehicles," 2015 IEEE Vehicle Power and Propulsion Conference (VPPC), Montreal, QC, 2015, pp. 1-6, doi: 10.1109/VPPC.2015.7352948.

[11] Texas Instruments, “Field Orientated Control of Three Phase AC-motors”, Literature number: BPRA073, December 1997

[12] Y. Olca, M. N. Ekım and A. F. Boz, "Investigation of the Effects of Current Measurement Methods on Servo Motor Dynamics," 2019 20th International Symposium on Power Electronics (Ee), Novi Sad, Serbia, 2019, pp. 1-5, doi: 10.1109/PEE.2019.8923238.

[13] J. Holtz, "Pulsewidth modulation-a survey," in IEEE Transactions on Industrial Electronics, vol. 39, no. 5, pp. 410-420, Oct. 1992, doi: 10.1109/41.161472.

[14] Mirahki, Hooshang. (2014). Torque Calculation in Interior Permanent Magnet Synchronous Machine Using Improved Lumped Parameter Models. Progress In Electromagnetics Research M. 39. 131-139. 10.2528/PIERM14093004.